J. Microbiol. Biotechnol. (2017), 27(2), 380–387
https://doi.org/10.4014/jmb.1606.06011

jmb

Characterization of Prototype Foamy Virus Infectivity in Transportin 3 Knockdown Human 293t Cell Line

Faysal Bin Hamid, Jinsun Kim, and Cha-Gyun Shin*

Department of Systems Biotechnology, Chung-Ang University, Ansung 17546, Republic of Korea

Received: June 8, 2016
Revised: August 25, 2016
Accepted: November 12, 2016

First published online
November 14, 2016

**Corresponding author*
Phone: +82-31-670-3067;
Fax: +82-31-675-3108;
E-mail: cgshin@cau.ac.kr

pISSN 1017-7825, eISSN 1738-8872

The foamy viruses are currently considered essential for development as vectors for gene delivery. Previous studies demonstrated that prototype foamy virus (PFV) can infect and replicate prevalently in a variety of cell types for its exclusive replication strategy. However, the virus-host interaction, especially PFV-transportin3 (TNPO3), is still poorly understood. In our investigation of the role of TNPO3 in PFV infection, we found lower virus production in TNPO3 knockdown (KD) cells compared with wild-type 293T cells. PCR analysis revealed that viral DNAs were mostly altered to circular forms: both 1-long terminal repeat (1-LTR) and 2-LTR in TNPO3 KD cells. We therefore suggest that TNPO3 is required for successful PFV replication, at least at/after the nuclear entry step of viral DNA. These findings highlight the obscure mysteries of PFV-host interaction and the requirement of TNPO3 for productive infection of PFV in 293T cells.

Keywords: Transportin-3, prototype foamy virus, 1-long terminal repeat, 293 T cell

Introduction

Foamy viruses (FVs), or spumaviruses, belong to the *Retroviridae* family. FVs are relatively complex and distinctive to other retroviruses for their aberrant replication pattern. Their dissemination has been reported generally in a wide range of non-human primates, such as monkeys, chimpanzees, cats, hamsters, and cattle, as well as humans infected from animal bites and scratches [1–4]. Interestingly, they exhibit persistent infection throughout the host life-cycle, showing severe cytopathic effects on adherent cells in vitro with giant multinucleated "foamy" syncytia and highly vacuolized appearance [2, 5]. Among them, prototype foamy virus (PFV), previously known as human foamy virus (HFV), was found initially from a Kenyan patient with nasopharynx carcinoma [6]. PFV has been reported to have a diverse scale of sensitivity to a wide range of cell lines in vitro [7].

The mechanism of nuclear import is not identical for all members of the *Retroviridae* family. Transportin 3 (TNPO3) or transportin-SR2 is a host transporting protein of mRNA splicing factors, especially phosphorylated serine/arginine rich proteins (SR proteins) to the nucleus. Several siRNA screening studies have demonstrated the importance of TNPO3 in HIV-1 replication, but the exact mechanism is still under controversy [8-10]. Shah *et al*. [11] reported that TNPO3 functions before nuclear entry, despite the fact other groups revealed its involvement at the nuclear step and/or the integration step [12–14]. Furthermore, it has been found that the capsid, not integrase (IN), determines the requirement of TNPO3 for HIV-1 replication [15]. However, nuclear transport of the viral genome occurs in G1/S phase-arrested cells, possibly using nuclear localization signals of Gag, Pol proteins, and IN [16–18]. Most recently it has been found that TNPO3 knockdown (KD) decreases PFV production in BHK-21 cells and interaction of TNPO3 with PFV IN, but not with Gag, indicating the requirement of IN-TNPO3 interaction in nuclear transport of the PFV pre-integration complex (PIC) [19]. PFV possesses both functional DNA and RNA [20, 21].

In this present study, we have investigated the sensitivity of PFV to human 293T cells, comparing to previously studied hamster cell line (BHK-21), and tested their virus production ability by transfection. We also demonstrated that PFV replication declines in the absence of TNPO3. Moreover, most of the viral DNAs are unable to integrate into the cellular genome, and formed higher unintegrated

DNAs (both 1-long terminal repeat (1-LTR) and 2-LTR) in TNPO3 KD cells. Interestingly, unintegrated DNAs were higher with time, which indicates an important role of TNPO3 in the PFV life-cycle.

Materials and Methods

Cell Culture

Baby hamster kidney cells BHK-21 (American Type Culture Collection, ATCC, USA) and 293T cells were cultured in Dulbecco's modified Eagle's medium (DMEM) supplemented with 10% heat-inactivated fetal bovine serum (Gibco Life Technologies, USA), 2 mM L-glutamine, 100 U/ml penicillin, and 100 μg/ml streptomycin. Foamy virus-activated β-Gal expression (FAB) cells (kind gift from Drs. Maxine L. Linial and Eun-Gyung Lee, Fred Hutchinson Cancer Research Center, USA) derived from the BHK-21 cell line bearing PFV LTR-β-galactosidase reporter cassettes were maintained in 100 μg/ml hygromycin.

Establishment of Stable TNPO3 Knockdown Cell Lines

TNPO3 expression was stably knocked down in BHK-21 and 293T cells by transfection with pGFP-V-RS vectors expressing shRNAs targeting hamster TNPO3 mRNA (sh72 (GI 362572)) and for human TNPO3, HuSH shRNA plasmid pGFP-V-RS (catalog #TR30007) from Origene (USA) as described previously [19]. Briefly, 4.8×10^5 cells were cultured on a 35 mm tissue culture plate, grown overnight at 37°C and 5% CO_2 in a humidified atmosphere, and then transfected with 2.8 μg of sh72 using the PEI transfection reagent following the manufacturer's instructions. The day after transfection, the transfected cells were grown and maintained in complete DMEM containing 10 μg/ml puromycin (Sigma, USA) for 2 weeks. Finally, the knockdown efficiency of TNPO3 was determined by western blotting.

Transfection and Production of Viral Stocks

PFVs were yielded by transient transfection of the pHSRV proviral plasmid [22] using the PEI transfection reagent as described previously [23]. Briefly, BHK-21 and 293T cells were grown on 100 mm tissue culture dishes. At the following day, the culture was at approximately 80% confluency and was transfected with 15 μg of pHSRV plasmid. After 48 h, the supernatant was harvested and stored at −80°C for further use. For high titer virus production, the transfected cells were detached from the bottom of the plate after the 2nd harvest of viruses. Then they were plated onto a 100 mm plate for about 3 weeks until all cells were died. During the period, the viruses produced from the transfected cells infect BHK-21 cells and produce more viruses. Supernatants were separated and pellets were crushed by freeze-thaw cycles. Then, both supernatants were centrifuged at 21,055 ×*g* at 4°C for 10 min to harvest viruses. The virus titer was measured with the FAB assay as described previously [24]. In brief, FAB cells are modified BHK-21 cells that are used for PFV infection experiments. FAB cells express β-galactosidase under the control of PFV LTR, which is transactivated by PFV Tas protein in relation to the level of virus replication. Approximately 4×10^5 FAB cells were infected with serially diluted PFV after 24 h of plating in 48-well culture plates. After 48 hours post-infection (hpi), cells were fixed with 0.2% glutaraldehyde, washed, and incubated 30 min with X-Gal (5-bromo-4-chloro-3-indolyl-β-D-galactopyranoside) substrate, and the number of blue cells was then counted.

Cell Viability Test

The viability of stable shRNA-mediated TNPO3 KD BHK-21 and 293T cells was evaluated by the MTT colorimetric dye reduction method as described previously [25]. Briefly, about 4×10^4 cells/well were grown on 96-well tissue culture plates for different times (12, 24, 48, or 72 h). After 48 h, 50 μl of 0.1mg/ml MTT (3-(4, 5-dimethylthiazol-2-yl)-2, 5-diphenyltetrazolium bromide; Sigma) was treated for 4 h. After discarding the MTT solution, cells were digested by DMSO and incubated in room temperature for 10 min. Then, absorbance at 595 nm was read by a microplate reader. Two independent experiments were performed for each replicate at the different time points.

Viral Infectivity Assay

Control 293T cells and TNPO3 KD cells were infected with cell-free culture supernatant at different dilutions in 48-well culture plates. At 12, 24, 48, and 72 hpi, supernatants were collected and centrifuged at 21,055 ×*g* at 4°C for 10 min. Heat-inactivated (100°C for 30 min) virus was used as the negative control. The infectivity of cell-free PFV supernatants was measured by the FAB assay described above.

Western Blot Assay

BHK-21 and 293T control and KD cells were lysed in RIPA buffer (150 mM NaCl, 50 mM HEPES, pH 7.4, 0.5% sodium deoxycholate, and 0.1% SDS) as described previously [26] and the protein concentration was measured using the Bradford assay. Equal amounts of total proteins were subjected to 12.5% SDS-PAGE and then transferred to Immobilon-P membranes (Millipore; USA) at 40 V for 4 h. The membranes were blocked for 2 h at room temperature with blocking buffer (5% nonfat dry milk, 0.1% Tween 20 in PBS). The membranes were incubated 12−16 h with rabbit polyclonal antibody against TNPO3 (1:500 dilutions; Abcam, UK) in blocking buffer. After three washes with PBS/0.1% Tween 20, the membranes were incubated with goat anti-rabbit IgG conjugated to horseradish peroxidase secondary antibody (1:10,000 dilution; Sigma) in blocking buffer for 1 h. The membranes were washed three times with PBS/0.1% Tween 20 and developed using a chemiluminescence (ECL) detection kit (Bionote, Korea). As an internal control, actin was probed with mouse monoclonal antibody against actin (1:5,000 dilution; Santa Cruz Biotechnology, USA) and then with anti-mouse IgG (1:10,000 dilution; Sigma).

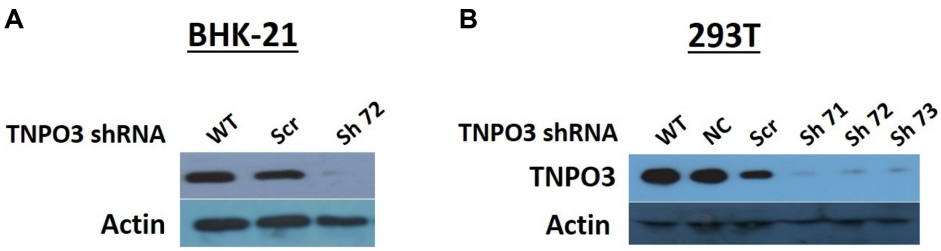

Fig. 1. Efficient knockdown of TNPO3 in both BHK-21 and human 293T cell lines by lentiviral vector-encoded shRNAs.
BHK-21 and 293T cells were plated at 70–80% confluent in 6-well plates. After 24 h, the shRNAs described below were transfected into both cells. At 48 h post-transfection, the cells were lysed and the TNPO3 protein expression was analyzed by western blotting. (**A**) TNPO3 KD in BHK-21 cells. WT: non-transfected; Scr: nonspecific shRNA; sh 72: sh 72 RNA transfected cells. (**B**) TNPO3 KD in 293T cells. WT: non-transfected; NC: Negative Control (vector itself); sh 71: sh 71 RNA; sh 72: sh 72 RNA; sh 73: sh 73 RNA transfected cells. β-Actin served as a loading control.

DNA Extraction and Purification

Both BHK-21 and 293T wild-type and KD cells were infected with PFV (moi 0.1) when the cells were about 70% confluent. After 2 h, 10% FBS-containing DMEM was changed. Then, the infected cells were incubated at 37°C in a 5% CO_2 atmosphere and harvested at 12, 24, 48, and 72 h post-infection. At particular time points, cells were washed twice with 1× PBS and lysed with the Hirt method as previously described [27]. Briefly, one million cells were washed once in PBS and mixed in 1 ml of 10 mM EDTA–10 mM Tris (pH 7.5); 10% sodium dodecyl sulfate (64 µl) was added, and the tubes were incubated on ice for 30 min. NaCl (3 M; 530 µl) was then added, and the tubes were incubated overnight at 4°C. For cellular DNA extraction to detect GAPDH DNA as a PCR control, we used an alternative lysis buffer: 10 mM Tris-Cl (pH 8.0), 0.1 M EDTA (pH 8.0), 0.5% (w/v) SDS. Then the cell-debris-containing tubes were centrifuged for 30 min at 4°C, 100 µg/ml of proteinase-K was added, and the samples were incubated at 37°C overnight. The DNAs were then extracted twice with a 1:1 mixture of phenol and chloroform, precipitated with ethanol, and digested with RNase A (final concentration 100 µg/ml).

Detection of Unintegrated DNAs

The following oligonucleotides were used for PCR (MyGenie96 Thermal Block; BioNEER): for 1-LTR circle: forward primer, 1-LTRS (5′-ATG GAA GCT TAT GGA CCT CAG-3′) and 1-LTRA (5′-CTT CAA CAT TAC TTC CTG AAG C-3′) [18]; for 2-LTR: 2-LTRS (5'-CAA TAA ACC GAC TTG ATT CGA GAA CCA ACT C-3′) and 2-LTRA (5'-CAT TTC CGC TTT CGG TGA CCA CTT TCC AGC-3′). The 20 µl reaction mixture contained 1× buffer, 0.5 mM deoxynucleoside triphosphates, 0.5 µM primers, 1U of Taq polymerase, and 100 ng DNA from each sample. Cycling conditions were as follows: 95°C for 30 sec, 60°C for 30 sec, and 72°C for 30 sec for 30 cycles (for 2-LTR) and 95°C for 1 min, 50°C for 1 min, and 72°C for 1 min (for 1-LTR), and a final extension at 72°C for 10 min. The PCR products were checked in 0.8% agarose gel.

Separately, glyceraldehyde-3-phosphate dehydrogenase (GAPDH) amplification was carried out as a PCR control for equal amounts of the target DNA using the following two primers: GAPDH-S, 5′-GGT TGC CAA ACC TTA TCA GAA ATG-3′; GAPDH-A, 5′-TTC ACC TGT TCC ACA GCC TTG-3′. The two primers amplified DNA fragment of 194 bp [28].

Results

Transfection of Different shRNAs Did Not Change Cell Viability

For knockdown of TNPO3, different shRNA plasmids (Scr, sh71, sh72, and sh73) were transfected into 293T cells and grown selectively in high concentration of puromycin-containing DMEM for 3 weeks. To evaluate the knockdown efficiency in 293T cells, cells extracts prepared from WT and KD cells were western blotted. The result showed TNPO3 was efficiently silenced in each shRNA-transfected cell (Fig. 1). In this experiment, BHK-21 was used as a control, as similar infectivity results were found previously.

MTT assay was used to determine the cell viability, detecting the mitochondrial activity. We tested the effect of transfection on cell viability using an MTT colorimetric assay. We found no notable differences between KD and control cells at the time of infection (Fig. 2). The result indicates transfection of the shRNA did not induce any cytotoxic effect that may influence PFV infection in further experiments.

PFV Production by Transfection Increases with Time

To check the transfection efficiency in BHK-21 and 293T cells, both cells were transfected with PFV producing plasmid pHSRV, because PFV infection in BHK-21 cells was previously studied and showed significant infection efficiency. After 12 hpi or earlier, both cells started to produce virus. At 1st harvest (12 h), virus titers were almost the same (2.5–3 × 10^3 PFU/ml) (Fig. 3). After more than 48 h, virus production increased gradually (about 5-fold).

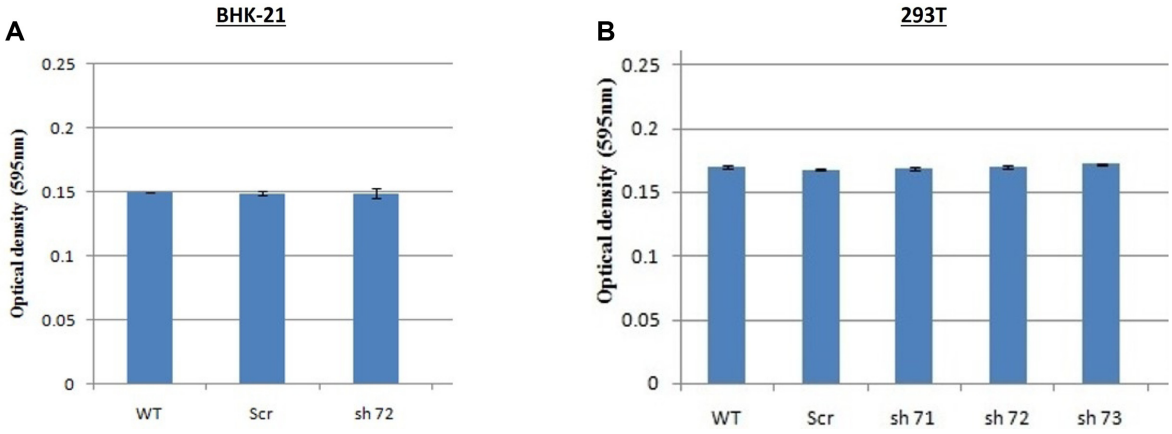

Fig. 2. Cell viability of WT cells and different 293T KD cells.

Cells were plated in 96-well plates and grown for 24 h at 37°C and 5% CO_2. Then, they were transfected with shRNAs. After 48 h, cell viability was monitored by MTT assay. (**A**) Viability of BHK-21 cells. Cells were transfected with no shRNA (WT), nonspecific shRNA (Scr), and sh 72 RNA (sh 72), respectively. (**B**) Viability of 293T cells. Cells were transfected with no shRNA (WT), nonspecific shRNA (Scr), sh 71 RNA (sh 71), sh 72 RNA (sh 72), and sh 73 RNA (sh 73), respectively. All experiments were performed three time independently. Data are presented as the mean ± SD.

However, the virus production peaked at 72 hpi in both cells. At this time-point, BHK-21 produced 3.55×10^5 PFU/ml and 293T produced 4.53×10^5 PFU/ml (Fig. 3). We also checked virus production from the two types of cells at 96 hpi. Although the virus production rate was increasing more (1×10^6 PFU/ml) in BHK-21 cells (data not shown), it was not possible to continue further because of the production of dead cells in 293T cells.

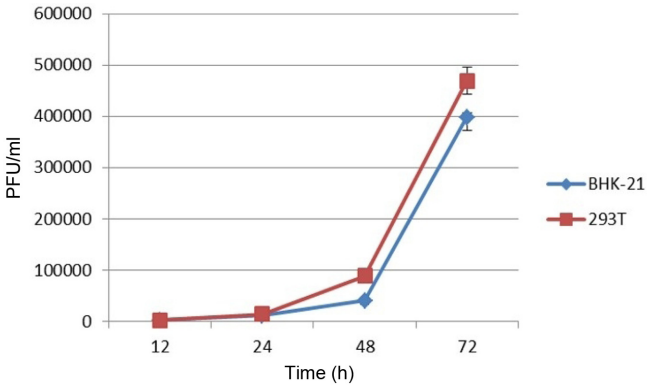

Fig. 3. Comparison of viral production between BHK-21 and 293T cells.

BHK-21 and 293T cells were plated in 100-mm tissue culture plates and transfected with pHSRV plasmid, respectively. At four different post transfection times (12, 24, 48, and 72 h), virus-containing supernatants were collected. Virus titers were evaluated by FAB assay. All experiments were performed three time independently. Data are presented as the mean ± SD.

Knockdown of TNPO3 in Human 293T Cells Decreases PFV Production

To study the potential role of TNPO3 in PFV infection and replication in 293T cells, TNPO3 expression was knocked down in BHK-21 (previously studied) and 293T cells by transfection of different shRNAs (Scr, sh71, sh72, and sh73). Scr (scrambled) shRNA targeted nonspecifically, and the other shRNAs specifically targeted TNPO3 transcripts. The efficiency of KD was verified by western blot technique of both wild-type and silenced cell extracts from established stable TNPO3 KD cell lines following puromycin (10 μg/ml) drug selection. Silencing with shRNA showed a remarkable reduction of TNPO3 expression in BHK-21 cells, but less reduced in 293T cell lines infected with PFV (moi 0.1) (data not shown). PFV production was evaluated by counting the blue cells (Fig. 4A) as described in Methods and Materials. At first harvest at 12 hpi, virus productions in sh72- and sh73-mediated KD cells were almost similar. On the other hand, the sh 73 knockdown effect was likely more severe, as it produced 3×10^3 PFU/ml viruses (Fig. 4B). At 24 hpi, the infection pattern was similar. However, PFV was produced 1.5–2-fold more than 12 hpi samples in both WT and TNPO3 KD cells (Fig. 4C). At 48 hpi, the knockdown mediated by sh71, 72, and 72 showed the most acute effect. PFV infection was decreased approximately 40% in 293T KD cells compared with WT cells (Fig. 4D). However, at 72 hpi, KD cells rescued the inhibitory effect caused by shRNAs to some extent, almost 20–22% (Fig. 4E). At this time-point, WT cells produced approximately 9×10^4 PFU/ml

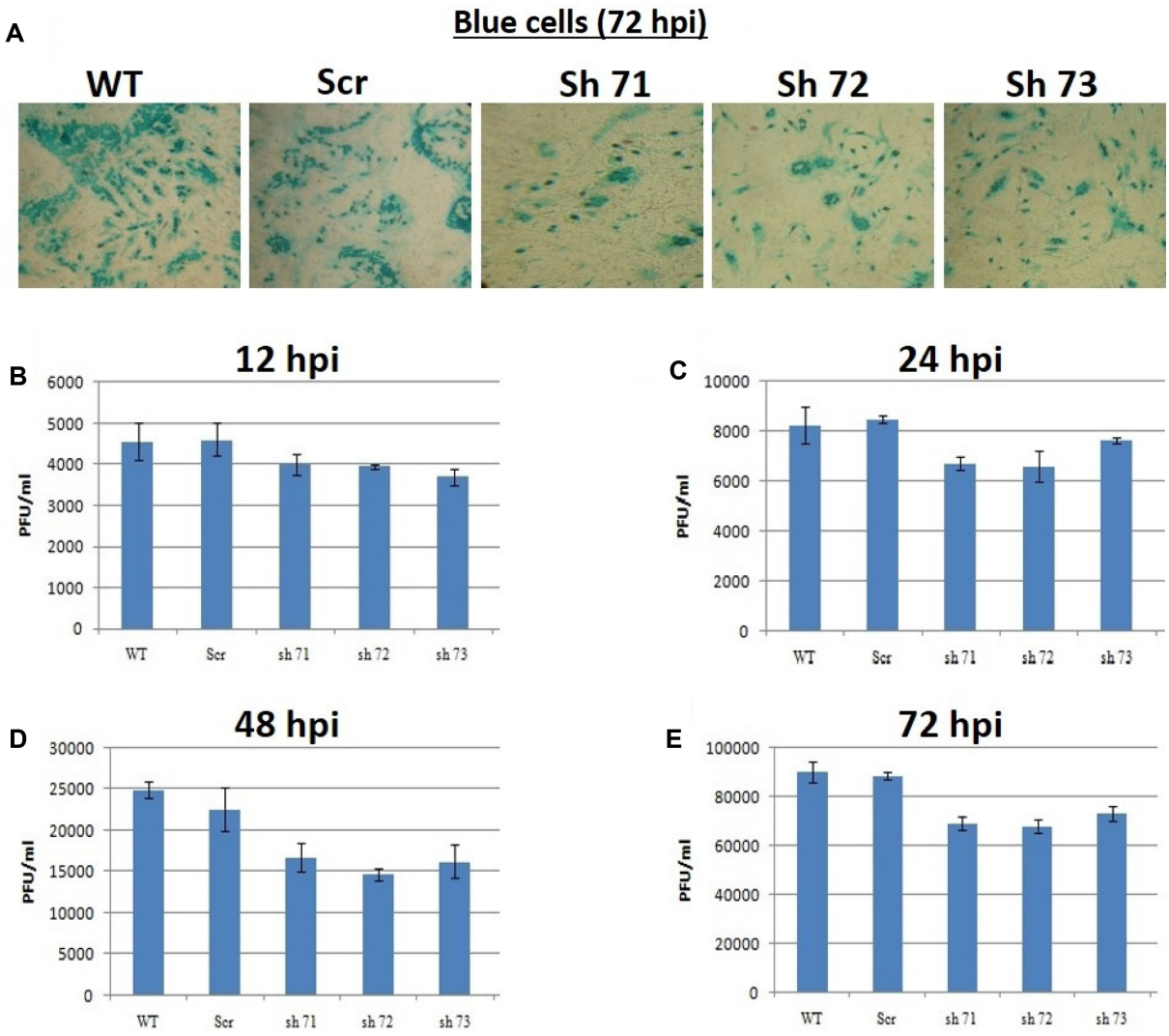

Fig. 4. TNPO3 knockdown (KD) in human 293T cells decreases PFV production.

293T cells were seeded in 35-mm plates and PFV viruses were infected at moi 0.1. At 12, 24, 48, and 72 hpi, the supernatants were collected and the virus titer was measured with FAB assay. As a negative control, we used heat-inactivated viruses for 1 h at 100°C. The negative control did not show any blue cells (data not shown). (**A**) Microscopic appearance of blue cells in FAB assay using viral supernatants of 72 hpi. About 1.2×10^5 FAB cells were seeded on 48-well plates and infected by viral supernatants of 72 hpi. After 48 h, cells were fixed and incubated with X-Gal for 4 h. (**B**–**E**) Viral titers. About 1.2×10^5 FAB cells were seeded on 48-well plates and infected by viral supernatants of 12 hpi (**B**), 24 hpi (**C**), 48 hpi (**D**), and 72 hpi (**E**), respectively. All experiments were performed three times independently. Data are presented as the mean ± SD.

whereas sh72-transfected cells produced the lowest viruses (6.7×10^4 PFU/ml).

Detection of Unintegrated DNAs (1-LTR and 2-LTR) in PFV-Infected Cells

To explore the role of TNPO3 during PFV infection, we challenged wild-type and TNPO3 KD cells with PFV for measuring the formation of circular unintegrated DNA species such as 1-LTR and 2-LTR at different time-points (12, 24, 48, and 72 hpi) (Fig. 5). The 2-LTR circles are commonly used as a marker for retroviral nuclear import. As it was previously shown that silencing of TNPO3 caused impairment in PFV infection [19], we investigated the formation of these two types of circular DNAs. After completion of making cDNA by reverse transcription, the reverse transcripts need to be imported into the nucleus where they integrate into the host genome or ligate to form 1-LTR and 2-LTR. To observe whether knockdown of

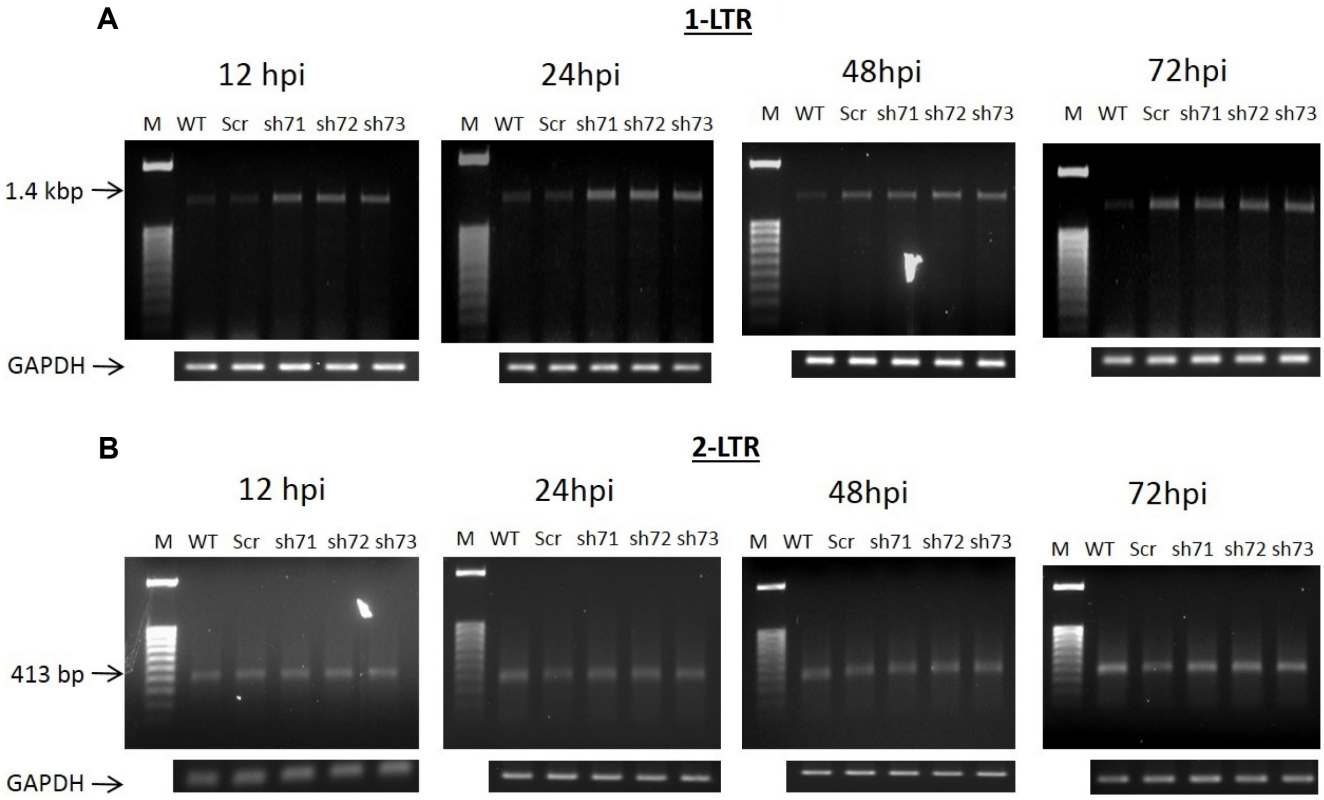

Fig. 5. TNPO3 knockdown increases unintegrated DNAs (1-LTR & 2-LTR) in PFV-infected 293T cells.
The 293T wild-type (WT) and TNPO3 KD cells (Scr, sh 71, sh 72, sh 73) were infected by PFV at moi 0.1. At 12, 24, 48, and 72 h post-infection, cells were washed and detached with trypsin. About 1×10^6 cells were lysed with the Hirt method to collect small DNA. (**A**) Detection of 1-LTR DNA. Formation of 1-LTR circles was detected by PCR. Primers (1-LTRs and 1-LTRA; see Materials and Methods for the detailed sequence) used for detecting 1-LTR were sequences designed from the *gag* and *bel* regions to identify the entire region yield from LTR-LTR. The product size was 1.4 kbp. (**B**) Detection of 2-LTR DNA. Formation of 2-LTR circles was detected by PCR. Primers (2-LTRS and 2-LTRA; see Materials and Methods for the detailed sequence) used for detecting 2-LTR were designed from the 3′ R and 5′ U3 regions to check only the LTR-LTR junction formation. The product size was 413 bp. Separately, in order to use a loading control of template DNA in the PCR, the same number of cells (1×10^6 cells) was lysed to collect cellular DNA. GADPH was amplified. M: 100 bp DNA marker.

TNPO3 influences the occurrence of the processes, we infected PFV in mock and TNPO3 KD cells. The PCR primers were commonly used sequences that flank the junction of the viral cDNA termini in both circular structures. As shown in Fig. 5A, at the first harvest time-point (12 hpi), knockdown of TNPO3, which blocks the import of viral DNA into the cellular genome, increased the amount of 1-LTR circles during PFV infection (Fig. 5A); with time (24, 48, and 72 hpi), the amount of 1-LTR increased in all the KD cells compared with WT cells. The increase of 1-LTR circles during HIV-1 infection of shRNA control cells in TNPO4 knockdown suggested that some of the viral DNAs that could not integrate were routed to the formation of 1-LTR circles. Similarly, we were also able to detect the formation of 2-LTR circles at the particular time points (Fig. 5B), but the differences among the WT and TNPO3 KD cells were not notable. Although 2-LTR formation was similar in TNPO3 KD cells and WT cells at each time-point (12, 24, 48, and 72 hpi) (Fig. 5B), the rate of 2-LTR formation was slightly increased at 48 hpi compared with 24 hpi, but the brightest PCR product at 72 hpi indicated the maximum 2-LTR formation at this time-point (Fig. 5B).

Discussion

To date, many studies have been conducted to find out the role of TNPO3 in different retroviral life-cycles [19, 29–31], but the exact role and molecular mechanism are still controversial. In this paper, we provided evidence of the engagement of TNPO3 in PFV infection. Previously, PFV showed dependency on TNPO3 for efficient infection in BHK-21 cells. Thus, to study the role of TNPO3 in PFV

replication in human 293T cells, we stably silenced TNPO3 using different shRNAs (sh 71, sh 72, sh73) (Fig. 1) and confirmed their viability compared with wild-type cells (Fig. 2). The infectivity pattern of PFV-infected KD cells clearly showed that TNPO3 KD cells significantly reduced PFV infection compared with wild-type cells (Fig. 4A), with almost 15–20% reduction of blue cells on average in every case. This result was also consistent to previous studies, where Ali *et al*. [19] showed approximately 50% reduction of PFV infection in BHK-21 cells. However, the virus production increased in KD cells with time, indicating the involvement of alternative mechanisms by which PFV evades from the adverse effect of TNPO3 depletion (4B, 4C, 4D, 4E). Although TNPO3 seems to be essential at the first hours of the PFV life-cycle, its activity may be reimbursed with time. The alternative mechanisms were likely the compensatory roles of other members of the karyopherin group or unknown.

We also investigated circular DNA formation in the wild type and three different KD cells. These special structures are generally formed when the viral cDNAs fail to incorporate with the cellular DNA. As unintegrated DNAs, especially 2-LTR, can be considered a marker for nuclear import of PIC, different groups have tried to find out the roles of different cellular factors indirectly by measuring 2-LTR copy number in cells. Similarly, finding out at which stage of PFV life TNPO3 functions, by analyzing 2-LTR formation pattern, is a purpose of this study, because some research groups reported its involvement at any step from uncoating to integration [11–14, 32]. Additionally, the capsid has been found as the determinant for utilization of TNPO3 during HIV-1 infection, as CA mutants and MLV/HIV-1 chimera viruses (*e.g*., E45A, N74D) showed altered capsid stability and less reliance on TNPO3 for infection [15]. A group reported that 2-LTR formation at 24 hpi in TNPO3 KD cells was not significantly changed compared with wild-type cells [13]. Previously, our group showed that TNPO3 depletion blocked nuclear import of IN, but not CA/NC [19]. Moreover, TNPO3 binds with PFV IN, but not with the CA/NC complex, which indicated altered dependency on TNPO3 of PFV [19]. Consistent with the data, we showed evidence of lower PFV infectivity as well as higher 2-LTR and 1-LTR formation in TNPO3 KD cells with time (Figs. 5A and 5B). Our results indicated that TNPO3 depletion caused impairment in PFV cDNA import in the nucleus, and its role is in the PFV life-cycle, probably during and/or after nuclear import. Moreover, the PCR products of both 1-LTR and 2-LTR were always higher and 1-LTR circles were generated more than 2-LTR circles at every time-point (Figs. 5A and 5B). The latter one was similar to the previous studies in HIV-1 replication [33]. Besides this, viral DNAs are less able to integrate with the cellular DNA in the absence of TNPO3. The PCR results reinforced the notion, because higher unintegrated DNA in TNPO3 KD cells is probably due to block at the nuclear transport of viral cDNAs in the cytoplasm. Furthermore, from our infectivity test, we also found higher infectivity of PFV at 72 hpi.

Combining the above data, we can assume that PFV commenced its replication before 12 hpi and boosted at 72 hpi by integration of its DNA into the 293T cellular DNA. However, after 48 hpi, since PFV-infected 293T cells showed some cytopathic effects, it indicates massive viral production in the cells as well as more 1-LTR and 2-LTR formation. Overall, these results indicate that 293T is a better cell line for PFV study, and TNPO3 is required to import the PFV genome into the nucleus for its replication.

Acknowledgments

This study was supported by a grant from the National Research Foundation of Korea (NRF), funded by the Korean government (NRF-2015R1D1A1A01059592).

References

1. Bodem J, Löchelt M, Winkler I, Flower RP, Delius H, Flügel RM. 1996. Characterization of the spliced *pol* transcript of feline foamy virus: the splice acceptor site of the pol transcript is located in *gag* of foamy viruses. *J. Virol*. **70:** 9024.
2. Callahan ME, Switzer WM, Matthews AL, Roberts BD, Heneine W, Folks TM, *et al.* 1999. Persistent zoonotic infection of a human with simian foamy virus in the absence of an intact *orf-2* accessory gene. *J. Virol*. **73:** 9619-9624.
3. Erlwein O, McClure MO, 2010. Progress and prospects: foamy virus vectors enter a new age. *Gene Ther*. **17:** 1423-1429.
4. Schweizer M, Turek R, Hahn H, Schliephake A, Netzer KO, Eder G, *et al.* 1995. Markers of foamy virus infections in monkeys, apes, and accidentally infected humans: appropriate testing fails to confirm suspected foamy virus prevalence in humans. *AIDS Res. Hum. Retroviruses* **11:** 161-170.
5. Keshet E, Temin HM. 1979. Cell killing by spleen necrosis virus is correlated with a transient accumulation of spleen necrosis virus DNA. *J. Virol.* **31:** 376-388.
6. Achong BG, Mansell PW, Epstein MA, Clifford P. 1971. An unusual virus in cultures from a human nasopharyngeal carcinoma. *J. Natl. Cancer Inst*. **46:** 299-307.
7. Hill CL, Bieniasz PD, McClure MO. 1999. Properties of human foamy virus relevant to its development as a vector

for gene therapy. *J. Gen. Virol.* **80:** 2003-2009.
8. Brass AL, Dykxhoorn DM, Benita Y, Yan N, Engelman A, Xavier RJ, *et al.* 2008. Identification of host proteins required for HIV infection through a functional genomic screen. *Science* **319:** 921-926.
9. Christ F, Thys W, De Rijck J, Gijsbers R, Albanese A, Arosio D, *et al.* 2008. Transportin-SR2 imports HIV into the nucleus. *Curr. Biol*. **18:** 1192-1202.
10. König R, Zhou Y, Elleder D, Diamond TL, Bonamy GM, Irelan JT, *et al.* 2008. Global analysis of host-pathogen interactions that regulate early-stage HIV-1 replication. *Cell* **135:** 49-60.
11. Shah VB, Shi J, Hout DR, Oztop I, Krishnan L, Ahn J, *et al.* 2013. The host proteins transportin SR2/TNPO3 and cyclophilin A exert opposing effects on HIV-1 uncoating. *J. Virol.* **87:** 422-432.
12. Cribier A, Ségéral E, Delelis O, Parissi V, Simon A, Ruff M, *et al.* 2011. Mutations affecting interaction of integrase with TNPO3 do not prevent HIV-1 cDNA nuclear import. *Retrovirology* **8:** 104.
13. De Iaco A, Santoni F, Vannier A, Guipponi M, Antonarakis S, Luban J. 2013. TNPO3 protects HIV-1 replication from CPSF6-mediated capsid stabilization in the host cell cytoplasm. *Retrovirology* **10:** 20.
14. Valle-Casuso JC, Di Nunzio F, Yang Y, Reszka N, Lienlaf M, Arhel N, *et al.* 2012. TNPO3 is required for HIV-1 replication after nuclear import but prior to integration and binds the HIV-1 core. *J. Virol.* **86:** 5931-5936.
15. Krishnan L, Matreyek KA, Oztop I, Lee K, Tipper CH, Li X, *et al.* 2010. The requirement for cellular transportin 3 (TNPO3 or TRN-SR2) during infection maps to human immunodeficiency virus type 1 capsid and not integrase. *J. Virol.* **84:** 397-406.
16. Patton GS, Erlwein O, McClure MO. 2004. Cell-cycle dependence of foamy virus vectors. *J. Gen. Virol.* **85:** 2925-2930.
17. Imrich H, Heinkelein M, Herchenrö der O, Rethwilm A. 2000. Primate foamy virus Pol proteins are imported into the nucleus. *J. Gen. Virol.* **81:** 2941-2947.
18. Saïb A, Puvion-Dutilleul F, Schmid M, Périès J, de Thé H. 1997. Nuclear targeting of incoming human foamy virus Gag proteins involves a centriolar step. *J. Virol*. **71:** 1155-1161.
19. Ali MK, Kim J, Hamid FB, Shin CG. 2015. Knockdown of the host cellular protein transportin 3 attenuates prototype foamy virus infection. *Biosci. Biotechnol. Biochem*. **9:** 1-9.
20. Moebes A, Enssle J, Bieniasz PD, Heinkelein M, Lindemann D, Bock M, *et al.* 1997. Human foamy virus reverse transcription that occurs late in the viral replication cycle. *J. Virol.* **71:** 7305-7311
21. Yu SF, Sullivan MD, Linial ML. 1999. Evidence that the human foamy virus genome is DNA. *J. Virol*. **73:** 1565-1572.
22. Lee HS, Kang SY, Shin CG. 2005. Characterization of the functional domains of human foamy virus integrase using chimeric integrases. *Mol. Cells* **19:** 246-255.
23. Mullers E, Stirnnagel K, Kaulfuss S, Lindemann D. 2011. Prototype foamy virus Gag nuclear localization: a novel pathway among retroviruses. *J. Virol.* **85:** 9276-9285.
24. Yu SF, Linial ML. 1993. Analysis of the role of the *bel* and *bet* open reading frames of human foamy virus by using a new quantitative assay. *J. Virol*. **67:** 6618-6624.
25. Armand-Ugon M, Gutierrez A, Clotet B, Este JA. 2003. HIV-1 resistance to the gp41-dependent fusion inhibitor C-34. *Antivir. Res.* **59:** 137-142.
26. Hossain A, Ali K, Shin CG. 2014. Nuclear localization signals in prototype foamy viral integrase for successive infection and replication in dividing cells. *Mol. Cells* **37:** 140-148.
27. Freed EO, Martin MA. 1996. Domains of the human immunodeficiency virus type 1 matrix and gp41 cytoplasmic tail required for envelope incorporation into virions. *J. Virol.* **70:** 341-351.
28. Ribeiro-Romao RP, Saavedra AF, De-Cruz AM, Pinto EF, Moreira OC. 2016. Development of real-time PCR assays for evaluation of immune response and parasite load in golden hamster infected by *Leishamnia braziliensis*. *Parasit. Vectors* **9:** 361-372.
29. Henderson BR, Percipalle P. 1997. Interactions between HIV Rev and nuclear import and export factors: the Rev nuclear localization signal mediates specific binding to human importin-beta. *J. Mol. Biol*. **274:** 693-707.
30. Matreyek KA, Engelman A. 2013. Viral and cellular requirements for the nuclear entry of retroviral preintegration nucleoprotein complexes. *Viruses* **5:** 2483-2511.
31. Truant R, Cullen BR. 1999. The arginine rich domains present in human immunodeficiency virus type 1 Tat and Rev function as direct importin beta-dependent nuclear localization signals. *Mol. Cell. Biol.* **19:** 1210-1217.
32. Schaller T, Ocwieja KE, Rasaiyaah J, Price AJ, Brady TL, Roth SL, *et al.* 2011. HIV-1 capsid-cyclophilin interactions determine nuclear import pathway, integration targeting and replication efficiency. *PLoS Pathog.* **7:** e1002439.
33. Kilzer JM, Stracker T, Beitzel B, Meek K, Weitzman M, Bushman FD. 2003. Roles of host cell factors in circularization of retroviral DNA. *Virology* **314:** 460-467.